



Remote sensing of upper canopy leaf area index and forest floor vegetation cover as indicators of net primary productivity in a Siberian larch forest

Keiji Kushida,¹ Alexander P. Isaev,² Trofim C. Maximov,² Gen Takao,³ and Masami Fukuda¹

Received 17 July 2006; revised 30 December 2006; accepted 19 January 2007; published 13 April 2007.

[1] In this study, we demonstrated that the leaf area index (LAI) and forest floor vegetation cover (FVC) are indicators of net primary productivity (NPP) in Siberian larch forest by considering forest biometric and CO₂ budget parameters. Further, we estimated the distributions of these indicators and the corresponding NPP using Landsat ETM+ imagery. This estimation was based on the spectral measurements of larch leaves and the forest floor and on radiative transfer modeling studies. The results revealed that the estimated and observed values of larch LAI and FVC were similar; however, the estimated NPP ($222 \pm 24 \text{ gC m}^{-2} \text{ yr}^{-1}$) was greater than that obtained from observations from meteorological towers and soil heterotrophic respiration values ($130\text{--}180 \text{ gC m}^{-2} \text{ yr}^{-1}$) at the study site. We present the geographical distributions of larch LAI, FVC, and annual NPP that are associated with the components of the CO₂ budget and spectral parameters, which will be used to conduct intercomparison studies in the future.

Citation: Kushida, K., A. P. Isaev, T. C. Maximov, G. Takao, and M. Fukuda (2007), Remote sensing of upper canopy leaf area index and forest floor vegetation cover as indicators of net primary productivity in a Siberian larch forest, *J. Geophys. Res.*, *112*, G02003, doi:10.1029/2006JG000269.

1. Introduction

[2] In Siberia and the Russian far east, larch forests occupy 263 million ha, thereby accounting for 52% of the total forest cover in the region [*Federal Service of Forest Management of Russia*, 1995] and 6.8% of the total forest area worldwide [*Food and Agriculture Organization of the United Nations*, 2001]. In the Sakha Republic (Yakutia), Russian Federation, larch forests occupy 109 million ha, accounting for 90% of the total forest cover in the region. These areas are underlain by continuous permafrost from the bottom of the seasonal thawing layer to depths of as much as 400–500 m. This prevents water infiltration, and large forest areas are preserved even under conditions of extremely low precipitation (200–300 mm/yr). The mean annual air temperature of Yakutsk has increased by 2.5°C in the last 100 years [*Romanovsky*, 2003] and is predicted to increase by 3–11°C in the next 100 years [*Sazonova et al.*, 2004]. This change is accompanied by changes in the larch forest and its CO₂ budget in a geographically distributed area that affect the atmospheric CO₂ concentration.

[3] In Canada, human-induced climate changes have had a detectable influence on the area that was burned by forest fires over recent decades [*Gillett et al.*, 2004], and forest fires themselves influence the changes in the boreal forest CO₂ budget [*Hinzman et al.*, 2003]. In particular, in Siberian larch forests, surface fires that burn only forest floors predominate over crown fires, while crown fires are more dominant in North America [*Wooster and Zhang*, 2004]. Disturbances in Siberian larch forest strongly alter the soil thermal and hydrological conditions; this is dependent on initial ice content in the soil and influences vegetation recovery [*Iwahana et al.*, 2005]. In order to estimate the changes in the CO₂ budget of the ecosystem before and after fires, the CO₂ budget in a geographically distributed area must be estimated.

[4] Remote sensing is the most promising method by which the geographical distribution of the CO₂ budget of terrestrial ecosystems and the changes it undergoes can be estimated. Remote sensing of net primary productivity (NPP) in North America was based on ecosystem modeling [*Goetz et al.*, 1999; *Kimball et al.*, 2000; *Liu et al.*, 2002]. These models were based on the leaf area index (LAI) and the fraction of absorbed photosynthetically active radiation (FAPAR) obtained from the remotely sensed normalized difference vegetation index (NDVI) for each vegetation type. The estimated LAI or FAPAR was combined with plant physiology models and climate data including temperature and precipitation. In order to estimate net ecosystem productivity (NEP) as a component of the ecosystem CO₂ budget, soil respiration was assumed to mainly include

¹Institute of Low Temperature Science, Hokkaido University, Sapporo, Japan.

²Institute for Biological Problems of Cryolithozone, Russian Academy of Science, Yakutsk, Russia.

³Hokkaido Research Center, Forestry and Forest Products Research Institute, Sapporo, Japan.

degradation of the litter from canopy foliage. *Kushida et al.* [2004] focused on the contribution of not only the canopy but also the forest floor mosses or lichens to the total NPP, and included the aerial estimation of mosses or lichens in the CO₂ budget of a spruce forest in interior of Alaska.

[5] Further, remote sensing of the ecosystem CO₂ budget distribution in forests in Siberia and the Russian Far East has been included in studies conducted on a global scale by using the NDVI spectral index [*Myneni et al.*, 2001; *Nemani et al.*, 2003; *Running et al.*, 2004; *Bunn and Goetz*, 2006]; however, these studies have not considered the ecosystem CO₂ budget at the regional or tree-species level. Boreal forests are characterized by the high contribution of forest floor NPP to the total NPP, but this differs depending on the tree species and site characteristics.

[6] Here we first demonstrate that the LAI of larch and forest floor vegetation cover (FVC) are indicators of the NPP of Siberian larch forest by considering forest biometric and CO₂ budget parameters. Second, we estimate the indicators and the corresponding NPP distribution using Landsat Enhanced Thematic Mapper Plus (ETM+) imagery.

2. Materials and Methods

2.1. Site Specifications

[7] Leaf and forest floor spectra were recorded in a 170-year-old larch forest (Neleger site, 62°19'N 129°31'E, 220 m asl) in the East Siberian taiga, which is located 35 km northwest of Yakutsk. Larch (*Larix cajanderi* Mayr.) is the dominant tree species, reaching heights of 20 m. More than 99% of the trees higher than 1 m are larch, present at a density of 0.2 trees/m². Up to a height of 10 cm, the understory is dominated by the evergreen shrub *Vaccinium vitis-idaea* L. Unvegetated portions with fallen larch leaves are widely present on the forest floor, although woody plants such as *Rosa acicularis* Lindl. and herbaceous plants such as *Limnas stelleri* Trin. occur in small portions. The topography is flat, and the soil type is silty loam.

[8] Summer and autumn Landsat ETM+ images of the study site were taken on 13 August 2000 and 3 October 2001 (path: 122 and row: 16). These images were overlaid and used for land cover classification. The larch forest was differentiated from other land categories such as pine and birch forests, fire scars, grasslands, water bodies, ice, and sand by maximum likelihood supervised classification of the two images. In the autumn image, the larch and birch forests are leafless. The larch forest area on the summer Landsat ETM+ image was used to estimate the geographical distribution of the NPP components. Atmospheric correction was performed using ATCOR2 for Erdas Imagine 8.7 (Leica Geosystems Corp., Heerbrugg, Switzerland) with the standard parameters (midlatitude summer, rural, 20.0 km scene visibility).

2.2. Spectral Measurements

[9] As described by *Kushida et al.* [2004], the forest floor vegetation cover (FVC), namely, *V. vitis-idaea* L. and the unvegetated portions with fallen and live larch leaves, were spectrally measured with a GER-2600 spectroradiometer (GER Corp., New York, United States) at a wavelength of 350–2500 nm in late July 2000 and 2001, respectively. For the FVC components, each reflectance of a 0.15-m diameter

circle to the nadir direction at wavelengths in the 1.5-nm interval in 350–1050 nm; the 11.5-nm interval in the 1050–2500 nm range was observed by alternately measuring the emissions from the object and from a standard reflectance Spectralon panel at least 5 times. A LI-COR integrating sphere (LI-1800-12) was attached to the spectroradiometer, and the method of *Daughtry et al.* [1989] was used to observe the reflectance and transmittance of the leaves set at the 14-mm diameter sample port.

[10] In late July 2001, in the same plot, the horizontal distribution of the forest floor plant species was mapped using 900 pictures of a 30 m × 30 m plot in the Neleger site; the field was described, and the cover ratios of the dominant species were determined.

2.3. Radiative Transfer Model

[11] The spectral data were used as input for a canopy radiative transfer model [*Kushida et al.*, 2004], which is based on the SAIL model [*Verhoef*, 1984] and a clumping index [*Chen et al.*, 2005], in order to calculate the variations in the relationships between the upper canopy LAI and the reflectance factors in the Landsat ETM+ bands depending on the change in FVC. The clumping index that denotes the inhomogeneity of leaf spatial distribution was set at 0.68 by adopting the value assigned to deciduous conifer forests in the Northern hemisphere in the global foliage clumping-index distribution estimated by *Chen et al.* [2005]. The leaf angle distribution was assumed to be spherical. The solar beam was assumed to be a specular radiation from a 45° zenith angle. The forest floor was modeled as a horizontal mixture of *V. vitis-idaea* and the unvegetated portion with fallen larch leaves.

2.4. Larch NPP

[12] The total NPP (gC m⁻² yr⁻¹) and NEP (gC m⁻² yr⁻¹) can be expressed as follows:

$$NPP = NPP_l + NPP_u, \quad (1)$$

$$NEP = NPP - SHR, \quad (2)$$

where NPP_l (gC m⁻² yr⁻¹) and NPP_u (gC m⁻² yr⁻¹) represent the NPP of the larch and the understory, respectively, and SHR (gC m⁻² yr⁻¹) represents soil heterotrophic respiration. On the basis of the mensuration of the larch (*L. gmelinii* (Rupr.) Rupr. and *L. cajanderi* Mayr.) forests in Yakutia, yield tables were prepared by *Usoltsev* [2002]. These tables include information on the age-related changes in the biomass of the stem (B_s , g/m²), foliage (B_f , g/m²), branch (B_b , g/m²), root (B_r , g/m²), and stand density (S , m⁻²) for each of the eight site indices that further indicate site condition and forest floor types. B_r can be further classified into fine root biomass (B_{fr} , g/m²) and coarse root biomass. NPP_l can be expressed as follows [after *Chen et al.*, 2002]:

$$\begin{aligned} NPP_l &= \Delta C + L_f + L_b + L_{fr} + M \\ &= \Delta C + r_f c_f B_f + r_b c_b B_b + r_{fr} c_{fr} B_{fr} + M, \end{aligned} \quad (3)$$

where ΔC (gC m⁻² yr⁻¹) is the carbon increment due to biomass increment; L_f (gC m⁻² yr⁻¹), L_b (gC m⁻² yr⁻¹),

Table 1. Parameters for CO₂ Budget Estimation^a

Components	Equations and Parameters	References
Biomass increment, ΔB^b	$\frac{B(A_i) - B(A_{i-1})}{A_i - A_{i-1}}$	Usoltsev [2002]
Foliage turnover rate, r_f	1.0 yr ⁻¹	...
Branch turnover rate, r_b	0.05 yr ⁻¹	Kanazawa and Osawa [1994], Harmon et al. [2000]
Fine root turnover rate, r_{fr}	0.16 yr ⁻¹	Matamala et al. [2003]
Mortality, M	$0.4 \frac{C(A_{i-1}) S(A_i) - S(A_{i-1})}{S(A_{i-1}) A_i - A_{i-1}}$	this study ^c
NPP of understory, NPP_u^d	57 gC m ⁻² yr ⁻¹	this study ^c
Soil heterotrophic respiration, SHR^f	49 gC m ⁻² yr ⁻¹	Sawamoto et al. [2001, 2003]
Specific leaf area, SLA	139.4 cm ² /g (d.w.)	Kanazawa and Osawa [1994]
Fine root biomass, B_{fr}^g	$B_r(-0.1351 \ln(B_r) + 1.3173)$ (g/m ²)	Chen et al. [2002], Kajimoto et al. [1999], Kajimoto et al. [2003]

^a $B(A_i)$, $C(A_i)$, and $S(A_i)$ denote biomass (g/m²), carbon amount (g/m²), and stand density (m⁻²), respectively, at age A_i (y). B_r denotes total root biomass (g/m²). The carbon content in foliage and fine roots and in other parts was assumed be 0.45 gC/g and 0.50 gC/g, respectively.

^bAge is $(A_i + A_{i-1})/2$ (years).

^cValue is calculated on the basis of work by Shvidenko and Nilsson [1998], Schulze et al. [1999], and Usoltsev [2002].

^dSite is the Neleger.

^eValue is calculated on the basis of work by Burton et al. [2002], Sawamoto et al. [2001, 2003], and Saito et al. [2005].

^fObservation is at the Neleger site.

^gRoot diameter is ≤ 5 mm.

L_{fr} (gC m⁻² yr⁻¹), and M (gC m⁻² yr⁻¹) are foliage litter fall, branch litter fall, fine root turnover, and mortality, respectively; r_f (yr⁻¹), r_b (yr⁻¹), and r_{fr} (yr⁻¹) are the turnover rates of foliage, branches, and fine roots, respectively; and c_f (gC/g), c_b (gC/g), and c_{fr} (gC/g) are the carbon contents of the foliage, branches, and fine roots, respectively. The carbon content of the foliage and fine roots and that of the other parts was assumed be 0.45 gC/g and 0.50 gC/g, respectively. The mortality at the age $(A_i + A_{i-1})/2$ (years) can be expressed as follows:

$$M\left(\frac{A_i + A_{i-1}}{2}\right) = \alpha_M \frac{C(A_{i-1}) S(A_i) - S(A_{i-1})}{S(A_{i-1}) A_i - A_{i-1}}, \quad (4)$$

where $C(A_i)$ (gC/m²) and $S(A_i)$ (m⁻²) denote the carbon amount and stand density, respectively, at age A_i (years), and α_M (gC/gC) denotes the coefficient of mortality. The NPP_i at each age for each of the eight site indices was calculated on the basis of data from the Usoltsev yield table and on the basis of r_f , r_b , r_{fr} , and α_M by using equation (3). The upper canopy LAI at each age for each of the eight site indices (LAI_i , m²/m²) was calculated as follows:

$$LAI_i = B_f \cdot SLA, \quad (5)$$

where SLA (cm²/g (d.w.)) is the specific leaf area of the larch; its value was fixed at 139.4 cm²/g (d.w.) as determined by Kanazawa and Osawa [1994].

[13] We then deduced the relationship between LAI_i and NPP_i for the East Siberian larch forest from the relationships between age and NPP_i or LAI_i by assuming r_f , r_b , r_{fr} , α_M , and SLA as constant values. The parameters of the CO₂ budget components were fixed as shown in Table 1. Larch is deciduous, and the foliage turnover rate (r_f) was set at 1.0 yr⁻¹.

[14] Gill and Jackson [2000] used several methods and found that the r_{fr} ranged from 0.8 yr⁻¹ in tropical regions to 0.4 yr⁻¹ at high latitudes. The adoption of these values

considerably increases the larch NPP in comparison to the values obtained from tower observations in Yakutia by Hollinger et al. [1998], Dolman et al. [2004], and Machimura et al. [2005]. On the other hand, Matamala et al. [2003] obtained a value of 0.16 yr⁻¹ for loblolly pine (*Pinus taeda* L.) in North Carolina by using depleted ¹³CO₂ under free-air CO₂ enrichment (FACE); this indicates the overestimation of r_{fr} by conventional methods. As an alternative, we adopted a value of 0.16 yr⁻¹ for r_{fr} .

[15] B_{fr} (fine root, ≤ 5 mm in diameter) was calculated from B_r by using the following equation [Chen et al., 2002]:

$$B_{fr} = B_r(-0.1351 \ln(B_r) + 1.3173). \quad (6)$$

This is common in spruce, pine, and boreal broadleaf forests. For larches (*L. gmelinii*) in Central Siberia [Kajimoto et al., 1999, 2003], B_{fr} was calculated from B_r by using this equation, and the values of B_{fr} were 526 g/m² and 445 g/m²; these values were similar to the actual values observed at the site, i.e., 590 g/m² and 410 g/m², respectively. In Siberia, both a macroscopic inventory [Shvidenko and Nilsson, 1998] and site-level observation [Schulze et al., 1999] revealed that mortality is equivalent to net stem wood growth. Assuming a value of 0.4 gC/gC for α_M , the Usoltsev yield table yields larch mortality in Yakutia as equivalent to its net stem wood growth on the basis of another assumption regarding the age distribution in Russian needleleaf forests [Shvidenko and Nilsson, 1996]. An r_b value of 0.05 yr⁻¹ was deduced by multiplying the value of the ratio of branch detritus to branch biomass in the 170-year-old larch forest in Yakutia [Kanazawa and Osawa, 1994] with the woody detritus decomposition rate of pine in Northwestern Russia, i.e., 0.05 yr⁻¹ [Harmon et al., 2000].

2.5. Forest Floor NPP

[16] For the following flux parameter determination, the hourly soil temperature at the soil surface and at a 10-cm depth in a *L. cajanderi* forest in Spasskaya Pad, Yakutia

Table 2. CO₂ Budget Components at the Neleger Site

	Value, gC m ⁻² yr ^{-1a}	References
Soil heterotrophic respiration, <i>SHR</i>	49	<i>Sawamoto et al.</i> [2001, 2003]
Total soil respiration, <i>TSR</i>	325	<i>Sawamoto et al.</i> [2001, 2003]
Larch root respiration, <i>RR_l</i>	148	<i>Kajimoto et al.</i> [1999], <i>Widen and Majdi</i> [2001], <i>Burton et al.</i> [2002], <i>Chen et al.</i> [2002], <i>Kajimoto et al.</i> [2003], <i>Saito et al.</i> [2005].
CO ₂ upward flux at the top of the understory, <i>F_{CO2}</i>	140	T. Machimura, personal communication, 2005
Understory root respiration, <i>RR_u</i>	128	this study ^b
Understory aboveground NPP, <i>ANPP_u</i>	185	this study ^c
Understory NPP, <i>NPP_u</i>	57	this study ^d

^aValue is revised by using temperature data in 1998.

^bValue is estimated by $RR_u = TSR - SHR - RR_l$.

^cValue is estimated by $ANPP_u = TSR - F_{CO_2}$.

^dValue is estimated by equation (7).

(1998) [*Ohta et al.*, 2001] was used; further, the anomalies estimated from the differences in the monthly mean air temperature between 1998 and a normal year were corrected. The fluxes for all months with the exception of May to September were assumed to be 0 gC m⁻² yr⁻¹. In 1998, the average monthly mean air temperature in May, June, July, August, and September and from May to September was 4.2, 18.7, 20.1, 16.9, 3.5, and 12.7°C, respectively, which was slightly warmer than that in a normal year.

[17] Soil heterotrophic respiration (*SHR*) at the Neleger site was fixed at 49 gC m⁻² yr⁻¹ based on calculations made by *Sawamoto et al.* [2001, 2003]. They related the total soil respiration (*TSR*) to the soil temperature on the basis of flux measurements using a closed-chamber method conducted at the Neleger site. They determined the *TSR*-*SHR* ratio as 15% by conducting flux measurements from soil samples that were collected at each soil horizon at the Neleger site and incubated under various temperature conditions. Plants on the soil surface were removed before setting the chamber for the measurement. The *TSR* at the Neleger site was estimated to be 361 gC m⁻² yr⁻¹ in 1998; it changed to 325 gC m⁻² yr⁻¹ in a normal year after the monthly air temperature anomalies between the two years were corrected.

[18] NPP of the forest floor (understory) vegetation (*NPP_u*) was then calculated as follows:

$$NPP_u = ANPP_u - RR_u = (TSR - F_{CO_2}) - (TSR - SHR - RR_l) = -F_{CO_2} + SHR + RR_l, \quad (7)$$

where *ANPP_u* (gC m⁻² yr⁻¹), *RR_u* (gC m⁻² yr⁻¹), *F_{CO2}* (gC m⁻² yr⁻¹), and *RR_l* (gC m⁻² yr⁻¹) are understory aboveground NPP, understory root respiration, CO₂ upward flux at the top of the understory (*F_{CO2}*), and larch root respiration (*RR_l*), respectively. From the relationship between temperature and flux [*Hollinger et al.*, 1998], *F_{CO2}* in a *L. gmelinii* forest in Yakutia was estimated to be 85 gC m⁻² yr⁻¹. The *F_{CO2}* at the Neleger site was 130 gC m⁻² yr⁻¹, as determined by tower observations conducted in 2004 (T. Machimura, personal communication, 2005); this value was revised to 140 gC m⁻² yr⁻¹ in a normal year after the monthly air temperature anomalies between the two years were corrected using the temperature-*F_{CO2}* relationship determined by *Hollinger et al.* [1998].

[19] *RR_l* at the Neleger site was fixed at 148 gC m⁻² yr⁻¹. *Burton et al.* [2002] observed broad, cross-species relationships between the fine root respiration rate, nitrogen content, and temperature as follows:

$$FRR = (-0.185 + 0.83N) \exp(0.092T), \quad (8)$$

where *FRR* (nmol CO₂·g⁻¹·s⁻¹) is the fine root respiration rate, *N* (%) is the fine root nitrogen content, and *T* (°C) is the ambient temperature. The *FRR* at the Neleger site was calculated using the larch *N* at the site and it was found to be 0.68% [*Saito et al.*, 2005]. Since the lateral roots of *L. gmelinii* in Siberia extend to a depth of 20 cm or lower below the ground surface [*Kajimoto et al.*, 1999], the ambient temperature was set as the soil temperature at a depth of 10 cm. Coarse root respiration rates were found to be 8–23% of the *FRRs* in the Boreal Ecosystem-Atmosphere Study (BOREAS) sites in Canada [*Widen and Majdi*, 2001] and were fixed at 15% of the *FRRs*. From equation (6) and the Usoltsev yield table, the coarse and fine root biomass at the Neleger site were estimated as 3060 g/m² and 780 g/m², respectively. This estimation was consistent with the results of a coarse root biomass study by *Kanazawa and Osawa* [1994]. On the basis of the relationship between temperature and root respiration, larch root respiration (*RR_l*) at the Neleger site was estimated as 148 gC m⁻² yr⁻¹ by weighing the coarse and fine root biomass.

[20] Thus, from equation (7), *NPP_u* was estimated to be 57 gC m⁻² yr⁻¹ at the Neleger site. Correspondingly, from the *TSR*, the *ANPP_u* and *RR_u* at the Neleger site were estimated to be 185 gC m⁻² yr⁻¹ and 128 gC m⁻² yr⁻¹, respectively. CO₂ budget components at the Neleger site are summarized in Table 2.

[21] Forest floor mapping and plant identification were carried out in the 30 m × 30 m plot at the Neleger site. On the basis of these studies, the plant cover ratios of *V. vitis-idaea*, other shrubs (*Rosa acicularis* Lindl., *Salix bebbiana* Sarg., *Betula platyphylla* Sukachev, etc.), herbaceous plants (*L. stelleri* Trin. etc.), and mosses (*Tomenthypnum nitens* (Hedw.) Loeske, *Polytrichum strictum* Brid., *Ptilidium ciliare* (L.) Hampe, etc.) were calculated and were found to be 41%, 4%, 7%, and 1%, respectively. Assuming that

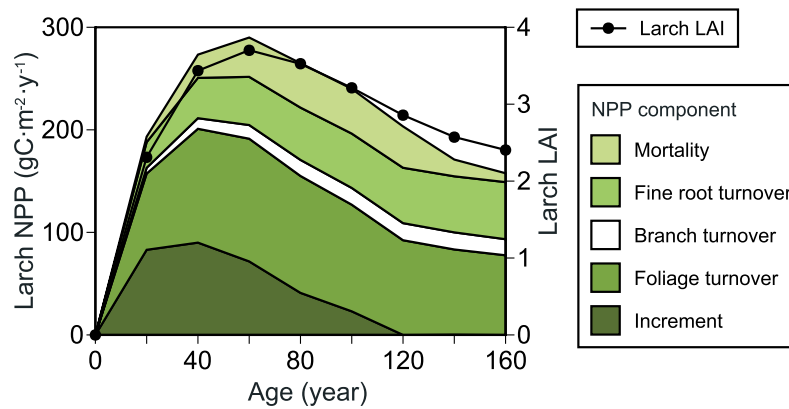


Figure 1. Changes in the components of the upper canopy (larch) LAI (LAI_t) and larch NPP (NPP_t) with the age of the larch forest (site index: *Vaccinium* type, V) in Yakutia. The solid circles indicate larch LAI (LAI_t). The areas within solid polygons indicate carbon increment due to biomass increment (ΔC), foliage turnover (L_f), fine root turnover (L_{fr}), and mortality (M) (arranged from darker to brighter shades); the white area indicates branch turnover (L_b).

the contributions of the mosses to the NPP_u are negligible and that the NPP of *V. vitis-idaea*, other shrubs, and the herbaceous plants per unit ground area is equivalent to that obtained at the Neleger site, which was $57 \text{ gC m}^{-2} \text{ yr}^{-1}$, the relationship between the forest floor vegetation cover FVC (%) and NPP_u was defined as follows:

$$NPP_u = 1.10FVC(\text{gC m}^{-2} \text{ yr}^{-1}). \quad (9)$$

2.6. Relationship Between NPP, Larch LAI, FVC, and Spectral Indices

[22] By using the radiative transfer model mentioned in section 2.3, we considered individual estimation of larch LAI and FVC from spectral indices. We then directly compared the estimation of the total NPP from $NDVI$ and the quotients of difference and summation of bands 4 and 2 $(B4 - B2)/(B4 + B2)$ and the $NDVI$ $(B4 - B3)/(B4 + B3)$ with that obtained from equation (11), in which the values of larch LAI and FVC were individually estimated from the spectral data. $B4$ (%) and $B3$ (%) are atmospherically corrected reflectance factors in Landsat ETM+ bands 4 and 3, respectively. $NDVI$ was calculated from the reflectance factors, and which differs from the $NDVI$ calculated from the spectral radiance or digital count values. In the simulation, we assumed that larch LAI and FVC are uniformly distributed from 0 to 4 and from 0% to 100%, respectively. $NDVI$, $(B4 - B2)/(B4 + B2)$, and the forest canopy reflectance factors were calculated for each larch LAI and FVC, assuming independent normal distributions of the larch leaf reflectance and transmittance and reflectances of *V. vitis-idaea* and fallen leaves with the averages and standard deviations obtained in the spectral measurements.

3. Results

3.1. Relationship Between NPP, Larch LAI, FVC, and Spectral Indices

[23] Analysis of the relationships between the upper canopy (larch) LAI and the larch NPP components showed

that the larch forest was characterized by a high contribution of foliage turnover to the larch NPP, and the LAI (LAI_t) and NPP (NPP_t) were highly correlated. The changes in the LAI and NPP components with the age of the larch forest (site index: *Vaccinium* type, V) are shown in Figure 1. The relationship between the LAI and NPP of the larch forest in Yakutia for the eight site indices are shown in Figure 2. The relationship between the upper canopy LAI and NPP was independent of the site index while that of spruce forests in North America was dependent on the site index [Kushida *et al.*, 2004, Figure 5]. The relationship between LAI_t and NPP_t was as follows:

$$NPP_t = 70.4LAI_t(\text{gC m}^{-2} \text{ yr}^{-1}) \quad (R^2 = 0.90). \quad (10)$$

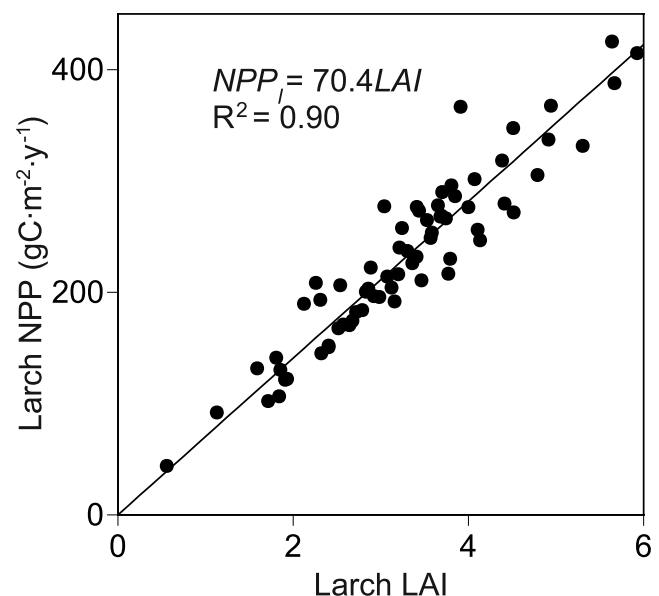


Figure 2. Relationship between the upper canopy (larch) LAI (LAI_t) and larch NPP (NPP_t). The solid circles correspond to each site index at each age.

Table 3. Spectral Characteristics of Forest Floor Components and Leaves of the Larch Forest in Landsat ETM+ Bands^a

Band	Wavelength	<i>V. vitis-idaea</i>	Fallen Leaves	Leaf reflectance	Leaf transmittance
1	0.45–0.52 μm	3.2 \pm 0.5	4.9 \pm 0.6	6.1 \pm 0.8	2.1 \pm 0.9
2	0.53–0.61 μm	8.8 \pm 1.1	9.4 \pm 1.1	13.2 \pm 1.8	7.7 \pm 0.9
3	0.63–0.69 μm	4.9 \pm 0.9	11.2 \pm 1.7	6.3 \pm 1.1	1.2 \pm 0.1
4	0.75–0.90 μm	41.3 \pm 3.8	24.1 \pm 3.2	48.8 \pm 5.1	38.8 \pm 3.7
5	1.55–1.75 μm	27.3 \pm 4.7	41.6 \pm 6.9	32.4 \pm 3.0	24.6 \pm 3.4
7	2.09–2.35 μm	25.0 \pm 10.9	47.5 \pm 9.8	58.6 \pm 10.2	22.8 \pm 14.7

^aValues are given as average \pm standard deviation, unit:%. The number of samples is 10 for forest floor reflectance and 14 for leaf reflectance and transmittance.

[24] The root mean square error (RMSE) of the NPP_t estimation was 26 $\text{gC m}^{-2} \text{yr}^{-1}$. From equations (1), (9), and (10), we obtain the following equation:

$$NPP = 70.4LAI_t + 1.10FVC + D(\text{gC m}^{-2} \text{yr}^{-1}), \quad (11)$$

where D ($\text{gC m}^{-2} \text{yr}^{-1}$) is a term that represents any unknown factors including climate factors. Equation (11) indicates that 1 (m^2/m^2) of LAI_t is equivalent to 64 (%) of FVC .

[25] From the radiative transfer analyses carried out using the component spectral characteristics observed, band 2 was found to be the most effective among the single bands, bi-band ratios, and quotients of bi-band difference and summation to obtain larch LAI. The reflectances from the larch canopy in band 2 were independent of the forest floor types. Table 3 shows the component spectral characteristics that were observed in the Landsat ETM+ bands. In band 2, *V. vitis-idaea* and the fallen leaves on the forest floor showed similar reflectances, and the reflectance factors of the larch forest in band 2 decreased as the larch LAI increased. In the other bands or any bi-band ratios, *V. vitis-idaea* and the fallen leaves showed different reflectances or exhibited lower sensitivities of the larch canopy reflectance to the larch LAI. For example, *V. vitis-idaea* had higher $NDVI$ and $(B4 - B2)/(B4 + B2)$ than those of the fallen leaves. Figure 3 shows the relationships of larch LAI and FVC with $NDVI$ and $(B4 - B2)/(B4 + B2)$. Both $NDVI$ and $(B4 - B2)/(B4 + B2)$ increased with an increase in the larch LAI and FVC, and the individual values of larch LAI and FVC were not well estimated using these spectral indices.

[26] The LAI value calculated from band 2 was used as the input for the radiative transfer model in the other bands. Among the single bands, bi-band ratios, and quotients of bi-band difference and summation, band 5 was the most sensitive to FVC. FVC was assigned a value under the assumption of independent normal distributions of the larch leaf reflectance and transmittance and the reflectances of *V. vitis-idaea* and the fallen leaves with the averages and standard deviations obtained in the spectral measurements. Figure 4 shows the relationships of larch LAI and FVC with bands 2 and 5, respectively.

[27] Individual values of larch LAI and FVC were not well estimated using $NDVI$ and $(B4 - B2)/(B4 + B2)$; however, these indices have the potential to estimate gross primary productivity as shown in previous studies. We compared the estimation of the total NPP by using $NDVI$ and $(B4 - B2)/(B4 + B2)$ with that by using equation (11) in

which the values of larch LAI and FVC were estimated using bands 2 and 5 under the assumptions mentioned in 2.6. Figure 5 shows the result of the simulation. The plateaus in the lower and higher NPPs in Figures 5a, 5b, and 5c resulted from the upper and lower limits of larch LAI and FVC that were set in the simulation. The RMSEs of the estimation using $NDVI$, $(B4 - B2)/(B4 + B2)$, and the function of bands 2 and 5 at 200 $\text{gC m}^{-2} \text{yr}^{-1}$ of NPP were 80, 75, and 48 $\text{gC m}^{-2} \text{yr}^{-1}$, respectively. Over the entire NPP range, the estimation using the function of bands 2 and 5 had a lower RMSE than that using $NDVI$ and $(B4 - B2)/(B4 + B2)$. This shows that NPP estimation using the function of bands 2 and 5 was more effective than that using the others, provided the spectral data are atmospherically corrected.

3.2. NPP Mapping

[28] Using equation (11) and the relationship of larch LAI and FVC with bands 2 and 5 (Figure 4), the geographical distributions of larch LAI, FVC, and the annual NPP were calculated using the August 2000 Landsat ETM+ imagery. The geographical distributions are shown in Figure 6. Evaluation by field observations at the Neleger site (Table 4, Neleger site) showed that the observed values of larch LAI and FVC were within the average \pm standard deviations of the estimated values of the two, respectively.

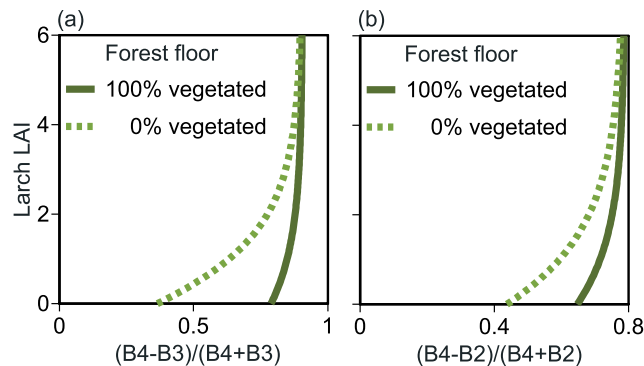


Figure 3. Relationships between the larch LAI (LAI_t), forest floor vegetation cover (FVC), and Landsat ETM+ spectral indices. (a) Landsat ETM+ $NDVI$ versus larch LAI (LAI_t); the solid and dotted lines indicate 100% and 0% FVC , respectively. (b) $(B4 - B2)/(B4 + B2)$ versus larch LAI (LAI_t); the solid and dotted lines indicate 100% and 0% FVC , respectively. $B2$ and $B4$ denote reflectance factors (%) in Landsat ETM+ bands 2 and 4, respectively.

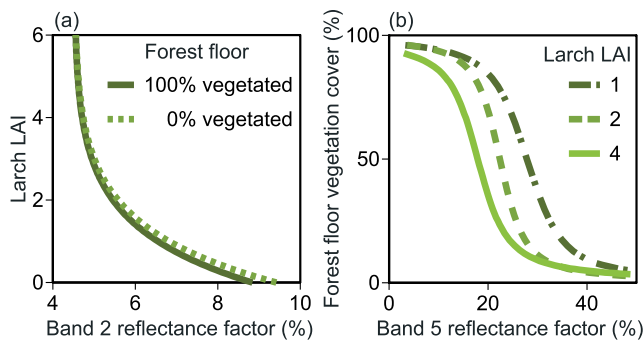


Figure 4. Relationships between larch LAI (LAI_l), forest floor vegetation cover (FVC), and reflectance factors. (a) Landsat ETM+ band 2 versus larch LAI (LAI_l); the solid and dotted lines indicate 100% and 0% FVC , respectively ($LAI_l = -1.321 \ln(0.2154B2 - 0.9698)$, $R^2 = 0.99$). (b) Landsat ETM+ band 5 versus FVC ; the chain, dotted, and solid lines indicate LAI_l values of 1, 2, and 4, respectively. ($FVC = -11.7B5 + 357 + E1$ ($LAI_l = 1$), $FVC = -20.8B5 + 491 + E2$ ($LAI_l = 2$), and $FVC = -73.0B5 + 1284 + E4$ ($LAI_l = 4$)), where $E1$, $E2$, and $E4$ are error functions and are 0 at $B5 = 50$ (%), and $B2$ and $B5$ denote reflectance factors (%) in Landsat ETM+ bands 2 and 5, respectively.

NPP was, however, overestimated. The average larch NPP that was estimated from the Landsat scene ($194 \pm 22 \text{ gC m}^{-2} \text{ yr}^{-1}$) (Table 4, $185 \text{ km} \times 185 \text{ km}$ area) was lower than that of the Neleger site by $30 \text{ gC m}^{-2} \text{ yr}^{-1}$.

[29] The relationship between the estimated NPP and NDVI showed that the range corresponding to each NDVI value was so wide that the NPP estimation by the NDVI could show different results from that by the individual estimation of larch LAI and FVC. Figure 7 shows the relationship between the estimated NPP and the NDVI for larch forests observed using Landsat ETM+ imagery. The lattices of the low-probability densities in Figure 7 were caused by quantization of the imagery. There was a significant correlation between the estimated NPP (NPP ($\text{gC m}^{-2} \text{ yr}^{-1}$)) and NDVI ($NDVI$) ($NPP = 511NDVI - 236$, $R^2 = 0.17$), but the RMSE in the regression was $20 \text{ gC m}^{-2} \text{ yr}^{-1}$,

which was close to the standard deviation of the estimated NPP ($22 \text{ gC m}^{-2} \text{ yr}^{-1}$).

[30] Larch LAI and FVC estimated from the Landsat ETM+ imagery were correlated ($LAI_l = -4.35FVC + 4.68$, $R^2 = 0.71$), but the distributions of the FVC, larch LAI, and the corresponding NPP estimated from the Landsat ETM+ imagery (Figure 8), revealed that the variations in FVC contributed to those in NPP even if the larch LAI was constant. This was because the isograms of NPP were almost parallel to the regression line of the larch LAI-FVC relationship. Thus FVC influences the estimation of larch canopy NPP using Siberian imagery.

4. Discussion

[31] On the basis of forest biometric and CO_2 budget parameters, we found that the larch LAI and FVC are indicators of the annual NPP of Siberian larch forest. These indicators were related to Landsat ETM+ bands using a radiative transfer model and component spectral characteristics. The distributions of the LAI, FVC, and NPP were mapped using Landsat ETM+ imagery. Evaluation using field observations showed that the estimated and observed values of larch LAI and FVC were equivalent; however, the estimated NPP was greater than that obtained from observations from meteorological towers and the heterotrophic soil respiration at the study site.

[32] The overestimation of NPP appeared to be due to the inadequacy of parameters for forest biometry and the influence of FVC. The estimated NPP was greater than that observed even when the differences between the estimated and observed values of larch LAI and FVC were corrected. Nevertheless, the biometric and meteorological methods for CO_2 budget estimation are based on different frameworks, and a simple comparison is difficult. The meteorological method detects the year-to-year variation, while the biometric method indicates the average values in the last 10 to 100 years.

[33] The contributions of heterotrophic respiration to the total soil respiration of larch [Sawamoto *et al.*, 2003] and pine [Kelliher *et al.*, 1999; Santruckova *et al.*, 2003] forests in Siberia were smaller than those of the boreal forests in Canada and Sweden [Bond-Lamberty *et al.*, 2004]. However,

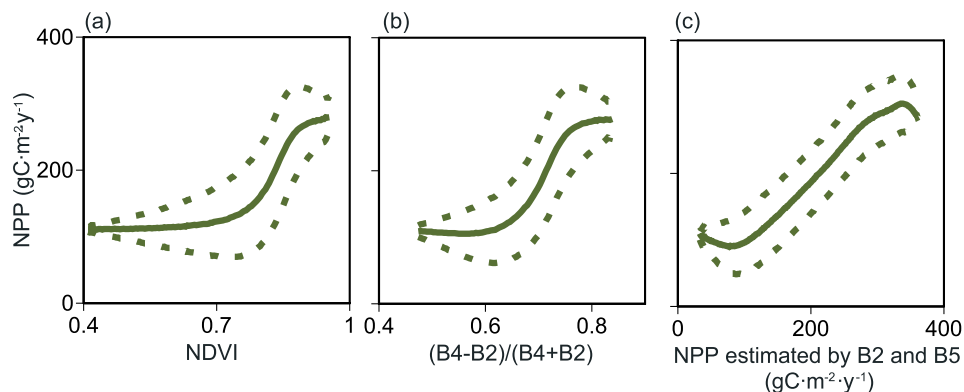


Figure 5. Simulation of NPP (NPP) estimation by (a) NDVI, (b) $(B4 - B2)/(B4 + B2)$, and (c) larch LAI (LAI_l) and forest floor vegetation cover (FVC) calculations by $B2$ and $B5$. The solid and dotted lines indicate average and average \pm S.D., respectively. In the simulation, LAI_l and FVC were assumed to be uniformly distributed from 0 to 4 and from 0% to 100%, respectively.

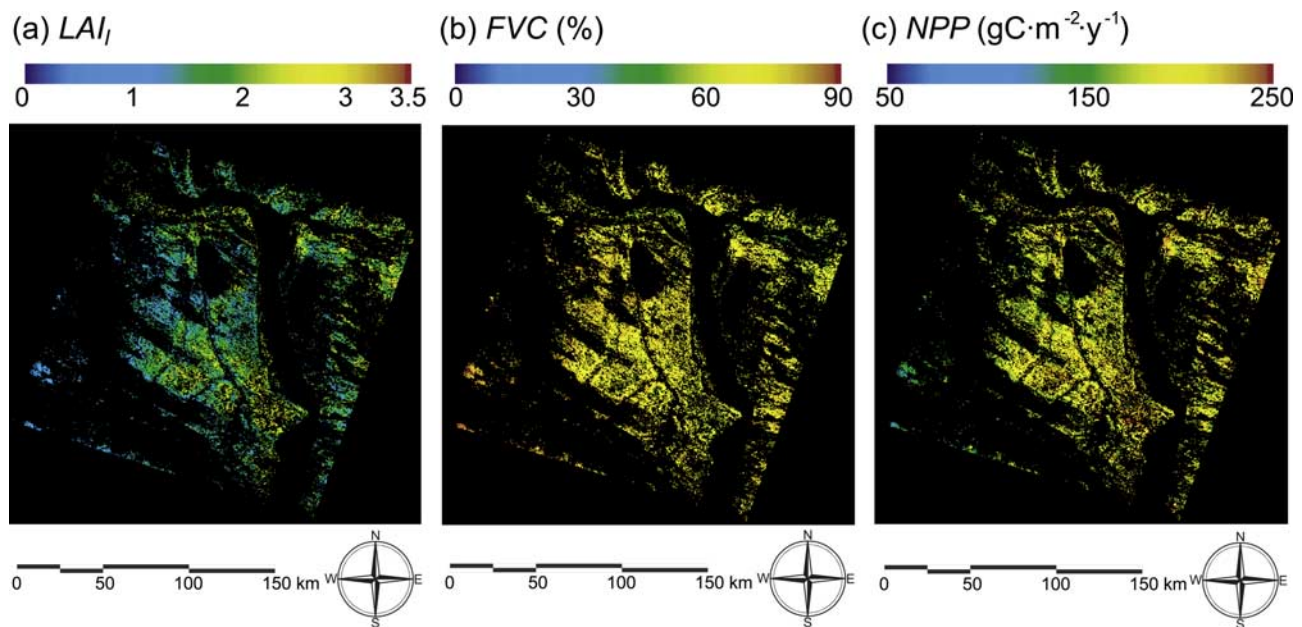


Figure 6. Geographical distributions of (a) upper canopy (larch) LAI (LAI_l), (b) forest floor vegetation cover (FVC), and (c) annual NPP (NPP) (Landsat ETM+ 122-16 on 13 August 2000; 61.8°N–63.9°N, 126.6°E–131.3°E; 300-m grid).

there are limited documented analyses of the soil heterotrophic respiration of the Siberian larch forest, and this makes evaluation difficult. Assuming that the soil heterotrophic respiration is greater by α $\text{gC m}^{-2} \text{yr}^{-1}$ than the observed value, NPP_u can be shown to increase by α $\text{gC m}^{-2} \text{yr}^{-1}$ from equation (9), and the NPP at the Neleger site is of the same value as that derived from equation (11).

[34] Mortality (M) that was set at 0.4 yr^{-1} (Table 1) was greater than or equal to that of spruce forests in Canada for which M ranged from 0.2 to 0.4 yr^{-1} [Chen *et al.*, 2002]. The r_b value that was set at 0.05 yr^{-1} was greater than that of spruce forests in Canada (r_b value, 0.024 yr^{-1}) [Chen *et al.*, 2002]. Assuming the mortality and branch turnover rate

to be 0.3 yr^{-1} and 0.024 yr^{-1} , respectively, the NPP at the Neleger site was found to decrease by $5 \text{ gC m}^{-2} \text{yr}^{-1}$ and $6 \text{ gC m}^{-2} \text{yr}^{-1}$, respectively.

[35] A possible reason for the overestimation may be that the parameters are barely measured. The r_{fr} value was set at 0.16 yr^{-1} by adopting the value in North Carolina that was determined using depleted $^{13}\text{CO}_2$, but r_{fr} is generally observed to decrease with latitude [Gill and Jackson, 2000]. If the r_{fr} at the Neleger site is assumed to be 0.08 yr^{-1} , the NPP at this site decreases by $14 \text{ gC m}^{-2} \text{yr}^{-1}$. In direct flux observations, it was difficult to distinguish between RR_l and $V. vitis-idaea$ root respiration. If 10% RR_l variation is assumed, the NPP at the Neleger site changes by

Table 4. Evaluation of the Estimation Using Field Observations

	Estimated ^a	Observed	References
		<i>Neleger Site</i>	
LAI	2.2 ± 0.3	2.4	Shibuya <i>et al.</i> [2004], Kanazawa and Osawa [1994]
FVC,%	61 ± 9	52 ^b	this study
NPP, $\text{gC m}^{-2} \text{yr}^{-1}$	222 ± 24	130–180 ^c	Machimura <i>et al.</i> [2005], Sawamoto <i>et al.</i> [2001, 2003]
		<i>185 km × 185 km Area</i>	
LAI	1.7 ± 0.4
FVC,%	69 ± 8
NPP, $\text{gC m}^{-2} \text{yr}^{-1}$	194 ± 22

^aValues are estimated from this study. For the Neleger site LAI and FVC, the averages \pm standard deviations were determined assuming the independent normal distributions of larch leaf reflectance and transmittance and the reflectances of *V. vitis-idaea* and fallen leaves with the averages and standard errors obtained in the spectral measurements. For the Neleger site NPP, the averages \pm standard deviations were determined using equations (11) and (2) assuming that the standard deviations of LAI and FVC and the RMS of larch NPP estimation from equation (10). For a $185 \text{ km} \times 185 \text{ km}$ area, the averages \pm standard deviations for a $300 \text{ m} \times 300 \text{ m}$ unit area were calculated using Landsat ETM+ (13 August 2000; path: 122, row: 16; 61.8°N–63.9°N, 126.6°E–131.3°E).

^bPercentages are as follows: 41% *V. vitis-idaea*, 4% other shrubs, and 7% herbaceous plants.

^cRange is obtained from tower flux observations and soil heterotrophic respiration at the Neleger site.

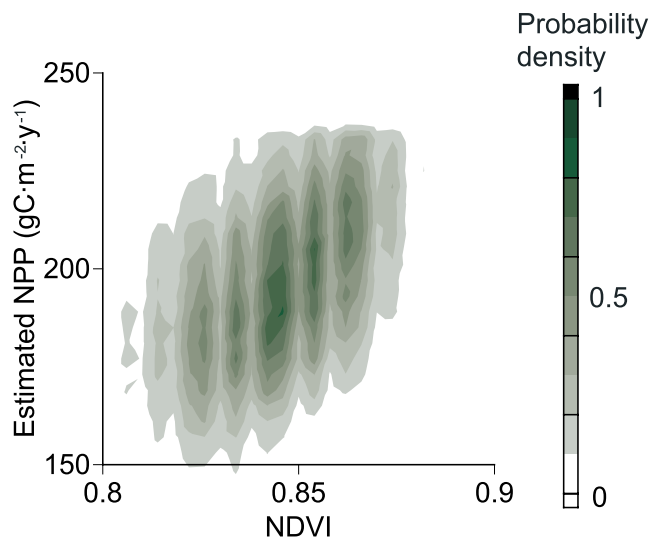


Figure 7. Relationship between NDVI and NPP estimated using the proposed method by Landsat ETM+ imagery. The probability densities were normalized by the maximum value.

15 $\text{gC m}^{-2} \text{yr}^{-1}$. There is little information on the specific leaf area (SLA) of Siberian larch trees, although SLA is one of the most important parameters in remote sensing and concerns the coefficient of the relationship between larch LAI and larch NPP. If a 10% SLA variation is assumed, the NPP at the Neleger site changes by 15 $\text{gC m}^{-2} \text{yr}^{-1}$. Therefore a combination of the variations in the above-mentioned parameters can account for the overestimation of NPP.

[36] The variations in turnover rates and understory NPP with those in the tree age and sites were not accounted for in this study because of the lack of observations. However, a strong relationship exists between larch LAI and larch NPP, and the relationship is based on foliage turnover that is equivalent to the upper layer LAI. When M , r_b , r_{fp} , and SLA were assumed to have the maximum values of 0.3 yr^{-1} , 0.024 yr^{-1} , 0.08 yr^{-1} , and 153.3 cm^2/g (d.w.), respectively, NPP_l was found to be $52.1LAI_l$ ($R^2 = 0.79$) with an RMSE of 32 $\text{gC m}^{-2} \text{yr}^{-1}$. NPP_u was implicitly estimated, and detailed observations in the future will lend better accuracy to this value. On the other hand, the CO_2 assimilation rate of *V. vitis-idaea* was equivalent to that of *L. gmelinii* based on the observations made in Yakutia by *Vygodskaya et al.* [1997]. The LAI of *V. vitis-idaea* was 67% of the LAI of larch in a 130-year-old *L. gmelinii* forest in Yakutia [*Kelliher et al.*, 1997]. These studies support the inclusion of NPP_u as an indicator of NPP. In the East Siberian larch forest, surface fires often occur. The frequency of surface fires characterizes the forest floor vegetation cover. The high variation in the forest floor vegetation cover that is caused by frequent surface fires in this region supports the assumption that the NPP_u per unit vegetated area is a constant proportional value.

[37] The estimation of the larch LAI from Landsat ETM+ band 2 was based on the observation that the reflectance factors of *V. vitis-idaea* and the fallen larch leaves in band 2 were similar, and the absorption by live larch leaves in

band 2 was 79% (Table 3). The reflectance factor of the live larch leaves was slightly greater than those of the fallen larch leaves and *V. vitis-idaea*. On the other hand, the distribution of the live larch leaves was observed to be three-dimensional, while those of *V. vitis-idaea* and the fallen larch leaves were horizontal. Owing to the high absorption of the live larch leaves, the increase in the larch LAI leads to an exponential increase in the absorption of the larch canopy in band 2, thereby decreasing the reflectance from the larch forest in band 2 (Figure 4a).

[38] The estimated NPP had a weak positive correlation with the NDVI for the larch forests that was observed using Landsat imagery (Figure 7). This suggests that NDVI is an indicator of larch NPP but does not perform as well as the estimation method used in this study. The estimation of the larch LAI and FVC as indicators of NPP is connected to the scientific bases obtained through biometric and meteorological studies. The negative correlation between the larch LAI and FVC that was estimated using Landsat imagery (Figure 8) can be explained by a reduction in the incident solar irradiance transmitted to the forest floor vegetation due to the increased larch LAI. The high contribution of FVC to the total NPP indicates that besides LAI, FVC is also an indicator of NPP. Other studies have noted similarly important influences of ground cover on boreal forest NPP [e.g., *Goetz and Prince*, 1996].

5. Conclusion

[39] We proposed several spectral indices to estimate the upper canopy LAI, forest floor vegetation cover, and NPP distributions of larch forests in East Siberia based on biometric analyses of the CO_2 budget, spectral measurements of the larch leaf and forest floor components, and radiative transfer modeling. Further, we evaluated the estimates using observations of field LAI, FVC, and meteorological CO_2 budgets. LAI has been estimated by remote

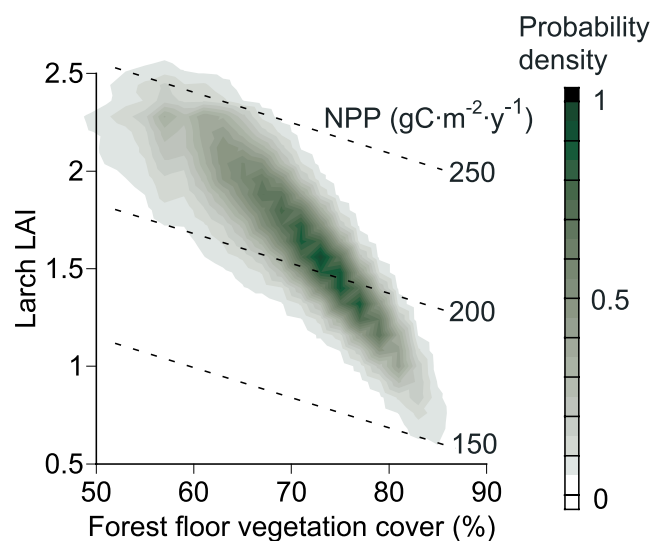


Figure 8. Relationship between the forest floor vegetation cover (FVC), larch LAI (LAI_l), and NPP estimated using Landsat ETM+ imagery. The probability densities were normalized by the maximum value. The dotted lines denote isograms of the estimated NPP.

sensing in many previous studies, but the relationship between LAI and the NPP components has rarely been studied at an individual tree-species level. Thus far, observations of the NPP of forest floor vegetation have been restricted to species such as mosses and lichens. This study includes assumptions for NPP component estimation, but comparisons of ecological and physiological studies using the results of this study may lead to further advancement in both these areas of research.

Notation

NPP	net primary productivity (NPP), $\text{gC m}^{-2} \text{yr}^{-1}$.
NEP	net ecosystem productivity (NEP), $\text{gC m}^{-2} \text{yr}^{-1}$.
NPP_l	net primary productivity (NPP) of larch, $\text{gC m}^{-2} \text{yr}^{-1}$.
NPP_u	NPP of understory, $\text{gC m}^{-2} \text{yr}^{-1}$.
SHR	soil heterotrophic respiration, $\text{gC m}^{-2} \text{yr}^{-1}$.
B_s	biomass of stem, g/m^2 .
B_f	biomass of foliage, g/m^2 .
B_b	biomass of branches, g/m^2 .
B_r	biomass of root, g/m^2 .
B_{fr}	biomass of fine roots, g/m^2 .
S	stand density, m^{-2} .
ΔC	carbon increment due to biomass increment, $\text{gC m}^{-2} \text{yr}^{-1}$.
L_f	foliage litter fall, $\text{gC m}^{-2} \text{yr}^{-1}$.
L_b	branch litter fall, $\text{gC m}^{-2} \text{yr}^{-1}$.
L_{fr}	fine root turnover, $\text{gC m}^{-2} \text{yr}^{-1}$.
M	mortality, $\text{gC m}^{-2} \text{yr}^{-1}$.
r_f	turnover rate of foliage, yr^{-1} .
r_b	turnover rate of branches, yr^{-1} .
r_{fr}	turnover rate of fine roots, yr^{-1} .
c_f	carbon content of foliage, gC/g .
c_b	carbon content of branches, gC/g .
c_{fr}	carbon content of fine roots, gC/g .
A_i	age, years.
$B(A_i)$	biomass at age A_i , g/m^2 .
$C(A_i)$	carbon amount at age A_i , gC/m^2 .
$S(A_i)$	stand density at age A_i , m^{-2} .
α_M	coefficient of mortality, gC/gC .
SLA	specific leaf area, cm^2/g (d.w.)
LAI_l	upper canopy (larch) LAI, m^2/m^2 .
TSR	total soil respiration, $\text{gC m}^{-2} \text{yr}^{-1}$.
$ANPP_u$	understory aboveground NPP, $\text{gC m}^{-2} \text{yr}^{-1}$.
RR_u	understory root respiration, $\text{gC m}^{-2} \text{yr}^{-1}$.
F_{CO_2}	CO_2 upward flux at the top of the understory, $\text{gC m}^{-2} \text{yr}^{-1}$.
RR_l	larch root respiration, $\text{gC m}^{-2} \text{yr}^{-1}$.
FRR	fine root respiration rate, $\text{nmol CO}_2 \text{g}^{-1} \text{s}^{-1}$.
N	fine root nitrogen content, %.
T	ambient temperature, $^{\circ}\text{C}$.
FVC	forest floor vegetation cover, %.
D	disturbance term (unknown factors) for NPP estimation, $\text{gC m}^{-2} \text{yr}^{-1}$.
$NDVI$	normalized difference vegetation index determined by Landsat ETM+ imagery.

B_2 reflectance factor in Landsat ETM+ band 2, %.

B_3 reflectance factor in Landsat ETM+ band 3, %.

B_4 reflectance factor in Landsat ETM+ band 4, %.

B_5 reflectance factor in Landsat ETM+ band 5, %.

E_1 , E_2 , and E_4 error functions for forest floor vegetation cover estimation, %.

[40] **Acknowledgments.** We wish to thank A. Osawa of Kyoto University and the anonymous reviewers for their helpful suggestions as well as C. I. Maximov for field assistance. This study was supported by the Research Revolution 2002 (RR2002) program of the Japan Ministry of Education, Culture, Sports, Science and Technology (MEXT), Global Environment Research Fund (B-053) of the Japan Ministry of Environment, Core to Core Program of Japan Society for the Promotion of Science (JSPS), and the Core Research for Evolutional Science and Technology (CREST) program of the Japan Science and Technology Agency (JST).

References

- Bond-Lamberty, B., C. K. Wang, and S. T. Gower (2004), A global relationship between the heterotrophic and autotrophic components of soil respiration?, *Global Change Biol.*, *10*, 1756–1766.
- Bunn, A. G., and S. J. Goetz (2006), Trends in satellite-observed circumpolar photosynthetic activity from 1982 to 2003: The influence of seasonality, cover type, and vegetation density, *Earth Interact.*, *10*, 1–19, doi:10.1175/EI190.1.
- Burton, A. J., K. S. Pregitzer, R. W. Ruess, R. L. Hendrick, and M. F. Allen (2002), Fine root respiration rates in North American forests: Effects of nitrogen concentration and temperature across biomes, *Oecologia*, *131*, 559–568.
- Chen, J. M., C. H. Menges, and S. G. Leblanc (2005), Global mapping of foliage clumping index using multi-angular satellite data, *Remote Sens. Environ.*, *97*, 447–457.
- Chen, W. J., J. M. Chen, D. T. Price, and J. Cihlar (2002), Effects of stand age on net primary productivity of boreal black spruce forests in Ontario, Canada, *Can. J. For. Res.*, *32*, 833–842.
- Daughtry, C. S. T., L. L. Biehl, and K. J. Ranson (1989), A new technique to measure the spectral properties of conifer needles, *Remote Sens. Environ.*, *27*, 81–91.
- Dolman, A. J., T. C. Maximov, E. J. Moors, A. P. Maximov, J. A. Elbers, A. V. Kononov, M. J. Waterloo, and M. K. van der Molen (2004), Net ecosystem exchange of carbon dioxide and water of far eastern Siberian larch (*Larix cajanderii*) on permafrost, *Biogeosciences*, *1*, 133–146.
- Federal Service of Forest Management of Russia (1995), *Forest Fund of Russia (Data of the State Forest Fund Inventory According to the State by 1 January 1993)* (in Russian), Fed. Serv. of For. Manage. of Russia, Moscow.
- Food and Agriculture Organization of the United Nations (2001), Global forest resources assessment 2000 (FRA 2000), *FAO For. Pap.* 140, Food and Agric. Org. of the U. N., Rome.
- Gill, R. A., and R. B. Jackson (2000), Global patterns of root turnover for terrestrial ecosystems, *New Phytol.*, *147*, 13–31.
- Gillett, N. P., A. J. Weaver, F. W. Zwiers, and M. D. Flannigan (2004), Detecting the effect of climate change on Canadian forest fires, *Geophys. Res. Lett.*, *31*, L18211, doi:10.1029/2004GL020876.
- Goetz, S. J., and S. D. Prince (1996), Remote sensing of net primary production in boreal forest stands, *Agric. For. Meteorol.*, *78*, 149–179.
- Goetz, S. J., S. D. Prince, S. N. Goward, M. M. Thawley, J. Small, and A. Johnston (1999), Mapping net primary production and related biophysical variables with remote sensing: Application to the BOREAS region, *J. Geophys. Res.*, *104*, 27,719–27,734.
- Harmon, M. E., O. N. Krankina, and J. Sexton (2000), Decomposition vectors: A new approach to estimating woody detritus decomposition dynamics, *Can. J. For. Res.*, *30*, 76–84.
- Hinzman, L. D., M. Fukuda, D. V. Sandberg, F. S. Chapin III, and D. Dash (2003), FROSTFIRE: An experimental approach to predicting the climate feedbacks from the changing boreal fire regime, *J. Geophys. Res.*, *108*(D1), 8153, doi:10.1029/2001JD000415.
- Hollinger, D. Y., et al. (1998), Forest-atmosphere carbon dioxide exchange in eastern Siberia, *Agric. For. Meteorol.*, *90*, 291–306.
- Iwahana, G., T. Machimura, Y. Kobayashi, A. N. Fedorov, P. Y. Konstantinov, and M. Fukuda (2005), Influence of forest clear-cutting on the thermal and

- hydrological regime of the active layer near Yakutsk, eastern Siberia, *J. Geophys. Res.*, *110*, G02004, doi:10.1029/2005JG000039.
- Kajimoto, T., Y. Matsuura, M. A. Sofronov, A. V. Volokitina, S. Mori, A. Osawa, and A. P. Abaimov (1999), Above- and below-ground biomass and net primary productivity of a *Larix gmelinii* stand near Tura, central Siberia, *Tree Physiol.*, *19*, 815–822.
- Kajimoto, T., Y. Matsuura, A. Osawa, A. S. Prokushkin, M. A. Sofronov, and A. P. Abaimov (2003), Root system development of *Larix gmelinii* trees affected by micro-scale conditions of permafrost soils in central Siberia, *Plant Soil*, *255*, 281–292.
- Kanazawa, Y., and A. Osawa (1994), Biomass of a *Larix gmelinii* (Rupr.) Litv. stand in Spasskaya Pad, Yakutsk, in *Proceedings of the Second Symposium on the Joint Siberian Permafrost Studies between Japan and Russia in 1993*, edited by G. Inoue, pp. 153–158, Natl. Inst. for Environ. Stud., Tsukuba, Japan.
- Kelliher, F. M., et al. (1997), Evaporation from an eastern Siberian larch forest, *Agric. For. Meteorol.*, *85*, 135–147.
- Kelliher, F. M., et al. (1999), Carbon dioxide efflux density from the floor of a central Siberian pine forest, *Agric. For. Meteorol.*, *94*, 217–232.
- Kimball, J. S., A. R. Keyser, S. W. Running, and S. S. Saatchi (2000), Regional assessment of boreal forest productivity using an ecological process model and remote sensing parameter maps, *Tree Physiol.*, *20*, 761–775.
- Kushida, K., Y. Kim, N. Tanaka, and M. Fukuda (2004), Remote sensing of net ecosystem productivity based on component spectrum and soil respiration observation in a boreal forest, interior Alaska, *J. Geophys. Res.*, *109*, D06108, doi:10.1029/2003JD003858.
- Liu, J., J. M. Chen, J. Cihlar, and W. Chen (2002), Net primary productivity mapped for Canada at 1-km resolution, *Global. Ecol. Biogeogr.*, *11*, 115–129.
- Machimura, T., Y. Kobayashi, G. Iwahana, T. Hirano, L. Lopez, M. Fukuda, and A. N. Fedorov (2005), Change of carbon dioxide budget during three years after deforestation in eastern Siberian larch forest, *J. Agric. Meteorol.*, *60*, 653–656.
- Matamala, R., M. A. Gonzalez-Meler, J. D. Jastrow, R. J. Norby, and W. H. Schlesinger (2003), Impacts of fine root turnover on forest NPP and soil C sequestration potential, *Science*, *302*, 1385–1387.
- Myneni, R. B., J. Dong, C. J. Tucker, R. K. Kaufmann, P. E. Kauppi, J. Liski, L. Zhou, V. Alexeyev, and M. K. Hughes (2001), A large carbon sink in the woody biomass of Northern forests, *Proc. Natl. Acad. Sci. U. S. A.*, *98*, 14,784–14,789.
- Nemani, R. R., C. D. Keeling, H. Hashimoto, W. M. Jolly, S. C. Piper, C. J. Tucker, R. B. Myneni, and S. W. Running (2003), Climate-driven increases in global terrestrial net primary production from 1982 to 1999, *Science*, *300*, 1560–1563.
- Ohta, T., T. Hiyama, H. Tanaka, T. Kuwada, T. C. Maximov, T. Ohata, and Y. Fukushima (2001), Seasonal variation in the energy and water exchanges above and below a larch forest in eastern Siberia, *Hydrol. Processes*, *15*, 1459–1476.
- Romanovsky, V. E. (Eds.) (2003), East Siberian air, ground temperature, and snow depth measurements, 1882–1994., Natl. Snow and Ice Data Cent., World Data Cent. for Glaciol., Boulder, Colo. (Available at <http://nsidc.org/data/ggd902.html>).
- Running, S. W., R. R. Nemani, F. A. Heinsch, M. S. Zhao, M. Reeves, and H. Hashimoto (2004), A continuous satellite-derived measure of global terrestrial primary production, *BioScience*, *54*, 547–560.
- Saito, H., M. Hattori, M. Suzuki, T. Shirota, M. Shibuya, R. Hatano, T. C. Maximov, and K. Takahashi (2005), Immediate changes in NEP following clear-cutting in a mature larch stand in eastern Siberia, in *Proceedings of the International Semi-open Workshop "C/H₂O/energy Balance and Climate Over Boreal Regions with Special Emphasis on Eastern Siberia,"* edited by T. C. Maximov et al., pp. 33–38, Inst. for Biol. Problems of Cryolithozone, Siberian Branch, Russ. Acad. of Sci., Yakutsk, Russia.
- Santruckova, H., et al. (2003), Microbial characteristics of soils on a latitudinal transect in Siberia, *Global. Change Biol.*, *9*, 1106–1117.
- Sawamoto, T., R. Hatano, M. Shibuya, K. Takahashi, A. P. Isaev, and R. M. Desyatkin (2001), CO₂, N₂O, and CH₄ fluxes from soil in Siberian-Taiga larch forests with different histories of forest fire, *Tohoku Geophys. J.*, *36*, 77–89.
- Sawamoto, T., R. Hatano, M. Shibuya, K. Takahashi, A. P. Isaev, R. V. Desyatkin, and T. C. Maximov (2003), Changes in net ecosystem production associated with forest fire in Taiga ecosystems, near Yakutsk, Russia, *Soil Sci. Plant Nutr.*, *49*, 493–501.
- Sazonova, T. S., V. E. Romanovsky, J. E. Walsh, and D. O. Sergueev (2004), Permafrost dynamics in the 20th and 21st centuries along the East Siberian transect, *J. Geophys. Res.*, *109*, D01108, doi:10.1029/2003JD003680.
- Schulze, E. D., et al. (1999), Productivity of forests in the Eurosiberian boreal region and their potential to act as a carbon sink—A synthesis, *Global Change Biol.*, *5*, 703–722.
- Shibuya, M., H. Saito, T. Sawamoto, R. Hatano, T. Yajima, K. Takahashi, J. Y. Cha, A. P. Isaev, and T. C. Maximov (2004), Time trend in above-ground biomass, net primary production, and carbon storage of natural *Larix gmelinii* stands in eastern Siberia, *Eur. J. For. Res.*, *7*, 67–74.
- Shvidenko, A., and S. Nilsson (1996), Expanding forests but declining mature coniferous forests in Russia, *Working Pap. WP-96-059*, 27 pp., Int. Inst. for Appl. Syst. Anal., Laxenburg, Austria.
- Shvidenko, A., and S. Nilsson (1998), Phytomass, increment, mortality and carbon budget of Russian forests, *Interim Rep. IR-98-105*, 29 pp., Int. Inst. for Appl. Syst. Anal., Laxenburg, Austria.
- Usoltsev, V. A. (2002), *Forest Biomass of Northern Eurasia: Mensuration Standards and Geography*, Scientific Issue, (in Russian), Ural Branch, Russ. Acad. of Sci., Yekaterinburg, Russia.
- Verhoef, W. (1984), Light scattering by leaf layers with applications to canopy reflectance modeling: The SAIL model, *Remote Sens. Environ.*, *16*, 125–141.
- Vygodskaya, N. N., et al. (1997), Leaf conductance and CO₂ assimilation of *Larix gmelinii* growing in an eastern Siberian boreal forest, *Tree Physiol.*, *17*, 607–615.
- Widen, B., and H. Majdi (2001), Soil CO₂ efflux and root respiration at three sites in a mixed pine and spruce forest: Seasonal and diurnal variation, *Can. J. For. Res.*, *31*, 786–796.
- Wooster, M. J., and Y. H. Zhang (2004), Boreal forest fires burn less intensely in Russia than in North America, *Geophys. Res. Lett.*, *31*, L20505, doi:10.1029/2004GL020805.

M. Fukuda and K. Kushida, Institute of Low Temperature Science, Hokkaido University, W8 N19, Kita-ku, Sapporo 060-0819, Japan. (kkushida@lowtem.hokudai.ac.jp)

A. P. Isaev and T. C. Maximov, Institute for Biological Problems of Cryolithozone, Russian Academy of Science, Lenin Avenue 41, Yakutsk 677891, Russia.

G. Takao, Hokkaido Research Center, Forestry and Forest Products Research Institute, Hitsujigaoka 7, Toyohira, Sapporo 062-8516, Japan.